Patch Antenna for Measuring the Internal Temperature of Biological Objects Using the Near-Field Microwave Radiometric Method

A Ubaichin[1,2], A Bespalko[3], A Filatov[4], E Alexeev[5], G Zhuk[5]

[1] Researcher, Institute of Non-destructive Testing, TPU, Tomsk, Russia
[2] Researcher, Special Design Bureau "Smena", TUSUR, Tomsk, Russia
[3] Leading researcher, Institute of Non-destructive Testing, TPU, Tomsk, Russia
[4] Professor, Special Design Bureau "Smena", TUSUR, Tomsk, Russia
[5] Engineer, Special Design Bureau "Smena", TUSUR, Tomsk, Russia
E-mail: dualog@mail.ru

Abstract. The near-field microwave antenna with central frequency of 2.23 GHz has been designed and manufactured to be used as a part of the medical microwave radiometric system. Experimental studies of the reflection coefficient in different parts of the human body were conducted using the developed antenna. The experimental studies were carried out in a group of volunteers with normal somatic growth. The results of the experiments were used to perform the analysis of the potential errors in the measurements obtained via the developed antenna.

1. Introduction

One of the most important tasks in early medical diagnosis is to determine an internal temperature of the biological tissue. Invasive methods of temperature measuring, not to mention the additional pain, are not effective and cause significant measurement errors. Widely used non-invasive methods are infrared and microwave imaging [1]. Infrared imaging is commonly used in medical practice; however, this method allows measuring only near-surface temperature. Therefore, it is impossible to fully determine the internal thermal processes. The internal temperature distribution with the accuracy level adequate for medical practice can be measured by methods based on microwave imaging [2].

The most widely used technique is the near-field microwave radiometry. In this case (figure 1), antenna *A* is in a direct contact with the human body, as a result, resolution increases, the reflection coefficient of the antenna-medium complex can be estimated, and the influence of the radio interference decreases. The accuracy in comparison with remote radiometric methods increases as well.

2. Antenna designing

The accuracy of the results obtained via the near-field microwave imaging depends both on the biological tissue structure under study and the absolute accuracy (and sensitivity) of the measuring device – microwave radiometer. Among different types of microwave radiometers [3–7] widely-spread in medical diagnosis, the microwave radiometer based on the modified zero measuring method is most advantageous [5]. This microwave radiometer allows measuring the internal temperature of biological objects and the reflection coefficient with no effect of the main destabilizing factors inherent in other types of radiometers. The main feature of the near-field microwave radiometric method is the need of impedance matching the antenna with the biological tissue.

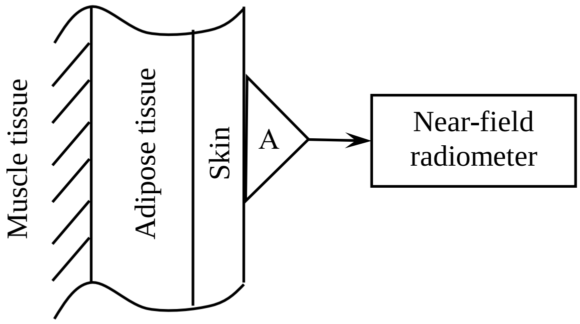

Figure 1. Biological tissue structure and the near-field radiometer for internal temperature measurement.

In [9], a comparative analysis of microwave antennas for the near-field radiometric method is provided. According to [9], waveguide antennas with regard to their main technical characteristics have a number of advantages (operating frequency range, matching with a layered medium), as compared to patch antennas. Technologically, patch antennas are most simple for manufacturing.

In [10–15], the authors consider various configurations of the radiating elements to achieve the required parameters: matching at the operating frequency range (reflection coefficient module is less than 0.5) [8], operating frequency width is at least 100 MHz.

Near-field patch antennas with circular radiating element are widespread. The design of these near-field antennas provides shielding, small size and ease of implementation by using a subtractive manufacturing technology in comparison with waveguide antennas. The technique of designing an antenna with a circular radiating element for the far zone is presented in [16]. A brief description of the methodology for development of the near-field antenna with a circular radiating element is as follows: dielectric substrates with low dielectric permittivity $\varepsilon = 2...3.8$ are used, thickness of dielectric substrates is at least 1 mm, location of the feeder in the radiating element is determined by the required impedance value.

A near-field patch antenna with a circular radiating element has been designed. The development of the mathematical model and structural modeling of the antenna were carried out to meet the requirements of the impedance matching of the antenna-feeder path with the biological tissue of the "skin - adipose tissue - muscle tissue" type.

The developed antennas are made of microwave dielectric material “FLAN” $\varepsilon = 2.2$, the substrate thickness is about 1 mm, the transverse dimension is about 13×13 mm, the central frequency is 2.23 GHz, and the 3 dB level bandwidth is 500 MHz.

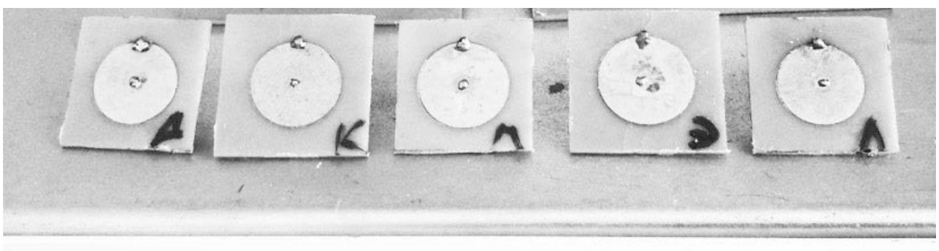

Figure 2. Designed models of the near-field antennas and the scalar network analyzer R2M-3200.

Variations in the biological tissue structure in the near-field measurements lead to antenna impedance mismatch. The influence of the biological tissue parameter variation (thicknesses of the skin, adipose and muscle tissue) on antenna matching has been evaluated at the design stage by using the computer-aided design CST Microwave Studio 2010. Some of the simulation results are shown in figure 3.

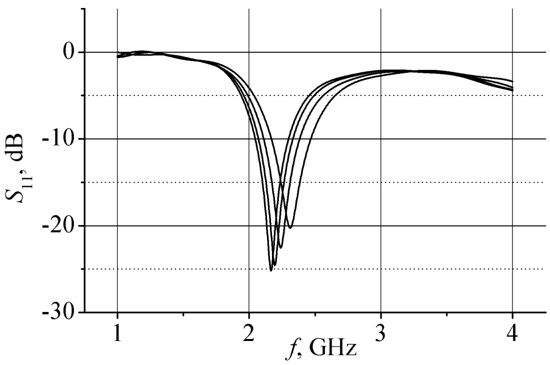

Figure 3. Effect of the changes in the layered medium thickness of the “skin-adipose tissue-muscle tissue” components on the S_{11} module.

The simulation results are obtained by varying the thicknesses of the biological medium layers within the following ranges: the thickness of the skin is from 0.5 to 2 mm, the thickness of the adipose tissue is from 0 to 20 mm, and the remaining space in the model has the dielectric parameters of the muscle tissue.

The experiments to study the reflection coefficient module of the biological medium were performed by using the designed antenna. The measurements were carried out in a group of volunteers with a normal somatic growth on particular parts of the body. The measurement results obtained using the scalar network analyzer R2M-3200 produced by JSC "Micran" are presented in Table 1.

Table 1. The results of the reflection coefficient module measurements in the frequency range from 2.18 to 2.28 GHz

Body area	The module of the reflection coefficient in the operating frequency band for the correlation number of the subjects, not more than								
	No.1	No.2	No.3	No.4	No.5	No.6	No.7	No.8	No.9
The inner side of forearm	0.107	0.075	0.184	0.110	0.200	0.104	0.110	0.095	0.101
The shoulder (outside)	0.158	0.127	0.135	0.127	0.170	0.115	0.124	0.117	0.130
The shoulder (inside)	0.193	0.188	0.190	0.178	0.202	0.098	0.175	0.198	0.180
The front surface of abdomen	0.316	0.124	0.191	0.210	0.305	0.256	0.180	0.230	0.185
The side surface of abdomen	0.101	0.03	0.120	0.130	0.280	0.090	0.129	0.189	0.123
The inner surface of thigh	0.203	0.185	0.212	0.199	0.253	0.150	0.207	0.200	0,175
The rear surface of lower leg	0.050	0.048	0.098	0,026	0,150	0.033	0.037	0.058	0.035
The larynx	0.079	0.084	0.070	0.090	0.124	0.050	0.048	0.073	0.034
The left half of chest	0.141	0.090	0.134	0.152	0.203	0.112	0.127	0.112	0.120
The right half of chest	0.125	0.085	0.147	0.167	0.234	0.090	0.130	0.124	0.110
The cheek area	0.251	0.199	0.208	0.203	0.280	0,199	0.153	0.235	0.205
The top of head area	0.177	0.162	0.180	0.170	0.180	0.165	0.179	0.150	0.139

There are two major factors affecting the accuracy of the biological tissue temperature profile measuring: the first factor is the efficiency of algorithms for inverse problem solving and the second one is absolute accuracy of the microwave radiometer used for measurements [17].

A mathematical model of the zero-type analog radiometer considered in [3] is limited to an ideal case with no insertion loss and with full reflection of the energy in the microwave switch. This model does not consider the impact of losses in the antenna-feeding path. In practice, the development of the microwave components with the parameters close to ideal ones is difficult.

The analysis shows that the influence of these factors decreases the accuracy of the measurement results, and at the level of the reflection coefficient module $R \geq 0.1$ (see Table 1) it causes significant errors.

To evaluate the efficiency of the developed antenna, the analysis of the errors in the noise temperature measurements of the biological tissue using the radiometer [5] based on the modified zero method measurements was performed. The input unit of the microwave radiometer [5] implemented in the block diagram is shown in figure 4.

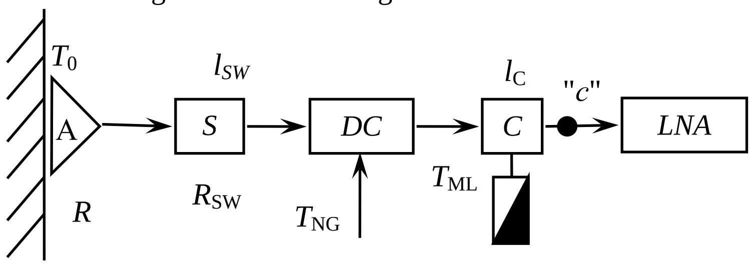

Figure 4. Block diagram of the input unit of the microwave radiometer: the tested object with temperature T_0, antenna *A*, microwave reflective switch *S*, directional coupler *DC*, circulator *C* and low noise amplifier *LNA*.

Figure 5 shows the timing diagram of the radiometer [18]. The pulse amplitude modulation signal t_{APM} (see figure 5) controls the switch (see figure 4) – in the time domain of the logical high signal t_{APM}, the switch is opened and the antenna is connected to the input of the *LNA*, in the time domain of the logical low signal t_{APM}, the switch is closed and the *LNA* receives signals T_{ML} and T_{NG} considering reflections in the closed switch [19]. The power transmission T_{NG} control is carried out by the pulse-width modulation signal t_{PWM}. The transfer of the signal T_{NG} occurs in the time domain of the logical high pulse-width modulation signal in the antenna waveguide towards the receiver, in the time domain of the logical zero, the signal T_{NG} is travels to the reflective switch. The pulse-width duration is changing until the condition of the equality of volt-second areas is fulfilled [5, 20, 21].

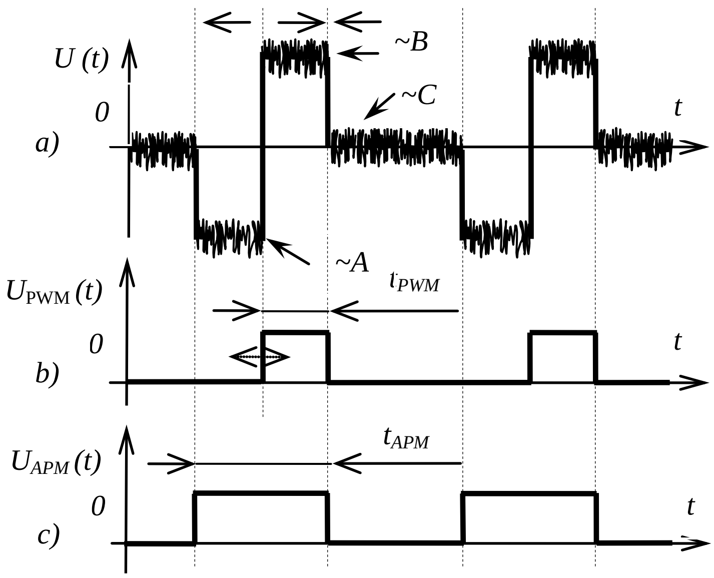

Figure 5. Timing diagrams of the zero-type radiometer: a) timing diagram of the logical signal at the input of the low noise amplifier at "c" point (see figure 4), the direction of the T_{NG} signal is indicated by arrows,
b) timing diagram of the amplitude-pulse modulation signal,
c) timing diagram of the pulse-width modulation signal.

In the following analysis, the efficiency of the near-field antenna is not considered. The near-field antenna together with the biological medium is characterized by the module of the power reflection coefficient R, the reflective switch is characterized by the transmission coefficient l_{SW} and by the module of the power reflection coefficient in a closed state R_{SW}, the transmission of the signal T_{NG} to the antenna waveguide is carried out by the directional coupler, and the matching load of the circulator (isolator operating mode) generates the T_{ML} signal.

In the above block diagram (see figure 4), the case of complete removal of the effect of antenna mismatching with the tested medium is realized only with full reflection from the closed switch disregarding the insertion loss in it. In practice, it is impossible to realize lossless switch and\or with full reflection of the signal from the closed input.

In the timing diagram a) (see figure 5), the levels of the signals are shown taking into account the imperfections of the reflective switch:

$$A \sim T_0 \cdot (1-R) \cdot l_{\mathrm{SW}} + R \cdot l_{\mathrm{SW}}^2 \cdot T_{\mathrm{NG}} + R \cdot l_{\mathrm{SW}}^2 \cdot T_{\mathrm{ML}} + (1-l_{\mathrm{SW}}) \cdot T_{\mathrm{ML}}$$

$$B \sim T_0 \cdot (1-R) \cdot l_{\mathrm{SW}} + T_{\mathrm{NG}} + R \cdot l_{\mathrm{SW}}^2 \cdot T_{\mathrm{ML}} + (1-l_{\mathrm{SW}}) \cdot T_{\mathrm{ML}}$$

$$C \sim R_{\mathrm{SW}} \cdot l_{SW} \cdot (T_{\mathrm{NG}} + T_{\mathrm{ML}}),$$

$$A \sim T_0 \cdot (1-R) \cdot l_{\mathrm{SW}} + R \cdot l_{\mathrm{SW}}^2 \cdot T_{\mathrm{NG}} + R \cdot l_{\mathrm{SW}}^2 \cdot T_{\mathrm{ML}} + (1-l_{\mathrm{SW}}) \cdot T_{\mathrm{ML}}$$

$$B \sim T_0 \cdot (1-R) \cdot l_{\mathrm{SW}} + T_{\mathrm{NG}} + R \cdot l_{\mathrm{NG}}^2 \cdot T_{\mathrm{ML}} + (1-l_{\mathrm{SW}}) \cdot T_{\mathrm{ML}}$$

$$C \sim R_{\mathrm{ML}} \cdot l_{ML} \cdot (T_{\mathrm{NG}} + T_{\mathrm{ML}})$$

where l_{SW} is the insertion loss in the reflective switch, R is reflection from the "object-antenna" border, T_{NG} is the noise temperature of the noise generator added to the antenna noise temperature T_A,
T_{ML} is the noise temperature of the matching load (see figure 1 and figure 4).

Let us write the expression to find the dependence of the pulse-width modulation signal on the medium noise temperature considering the data and the values of A, B, C levels provided in [7]

$$T_0 = \frac{(1+R) \cdot T_{\mathrm{ML}} \cdot (l_{\mathrm{SW}}-1) - (R - R_{\mathrm{SW}}) \cdot l_{\mathrm{SW}}^2 \cdot T_{\mathrm{ML}} + R_{\mathrm{SW}} \cdot T_{\mathrm{NG}} \cdot l_{\mathrm{SW}}^2}{(R-1) \cdot l_{\mathrm{SW}}} - \frac{t_{\mathrm{PWM}}}{t_{\mathrm{APM}}} \cdot \frac{T_{\mathrm{NG}} \cdot (1 + R \cdot l_{\mathrm{SW}}^2)}{(R-1) \cdot l_{\mathrm{SW}}}. \quad (1)$$

For the case of an ideal reflective switch (R_{SW}=1, l_{SW}=1), the expression (1) takes the form

$$T_0 = T_{\mathrm{ML}} + T_{\mathrm{NG}} - \frac{t_{\mathrm{PWM}}}{t_{\mathrm{APM}}} \cdot T_{\mathrm{NG}}. \quad (2)$$

Expression (2) is consistent with the data in [5] for idealized elements.

The modern microwave reflection switch has an insertion loss level of 0.01...0.1 and the reflection coefficient of 0.9...0.99 at the shortwave region of the *S*-range. Taking into account the data range of the reflection coefficient module (see Table 1 – the maximum antenna reflection coefficient R_{MAX}=0.316) and the range of the input module imperfections (insertion loss and not full reflection in the switch), determine the possible measurement error by using expression (1). In solving the inequality (3) obtained by (1) taking into account the range of values $0.9 \le l_{\mathrm{SW}} \le 0.99$, $0.9 \le R_{\mathrm{SW}} \le 0.99$ и $0 \le R_{MAX} \le 0.316$ for the dynamic measurement range of 10 K at the range boundaries l_{SW}, R_{SW}, R_{MAX}, the errors exceed the desired accuracy by more than one order of magnitude.

$$\Delta T \ge \frac{(1+R_{\mathrm{MAX}}) \cdot T_{\mathrm{ML}} \cdot (l_{\mathrm{SW}}-1) - (R_{\mathrm{MAX}} - R_{\mathrm{SW}}) \cdot l_{\mathrm{SW}}^2 \cdot T_{\mathrm{ML}} + R_{\mathrm{SW}} \cdot T_{\mathrm{NG}} \cdot l_{\mathrm{SW}}^2}{(R_{\mathrm{MAX}}-1) \cdot l_{\mathrm{SW}}} - \frac{t_{\mathrm{PWM}}}{t_{\mathrm{APM}}} \cdot \frac{T_{\mathrm{NG}} \cdot (1 + R \cdot l_{\mathrm{SW}}^2)}{(R_{\mathrm{MAX}}-1) \cdot l_{\mathrm{SW}}}, \quad (3)$$

The measurement accuracy ΔT=0.05 K is provided for the range of values of the antenna reflection coefficient module within the limits $0 \le R \le 0.316$ under the condition of $0.98 \le l_{\mathrm{SW}} \le 0.99$, $0.98 \le R_{\mathrm{SW}} \le 0.99$.

3. Conclusion

Thus, the developed antenna can be used for testing the biological tissue by the near-field microwave radiometer in case of using the microwave input unit with the reflection switch characteristics close to ideal parameters. If the input module characteristics do not provide the desired accuracy, it is necessary to use antennas that comply with the requirements for matching of the tested tissue (body area).

A single antenna can also be used if both the noise temperature and the reflection coefficient module are measured simultaneously with subsequent correction of the measurement results taking into account the influence of the reflection coefficient module.

This work was supported by The Ministry of Education and Science of the Russian Federation in part of the Science program.

References

[1] Hand J W, Van Leeuwen G M J, Mizushina S, Van De Kamer J B, Maruyama K, Suiura T, Azzopardi D V and Edwards AD (2001) Monitoring of deep brain temperature in infants using multi-frequency microwave radiometry and thermal modelling *Phys. Med. Biol.* **46**(7) 1885–1903

[2] Rosen A, Stuchly M A and Vander Vorst A (2002) Applications of RF/microwaves in medicine *IEEE Transactions on Microwave Theory and Techniques* **50**(3) 963–974

[3] Oikonomou A, Karanasiou I S and Uzunoglu N K (2010) Phased-array near field radiometry for brain intracranial applications *Progress in Electromagnetics Research* **109** 345–360

[4] Karanasiou I S, Uzunoglu N K and Papageorgiou C C (2004) Towards functional noninvasive imaging of excitable tissues inside the human body using focused microwave radiometry *IEEE Trans. Microwave Theory Tech.* **52**(8 II) 1898–1908

[5] Yablonskiy D A, Ackerman J J H and Raichle M E (2000) *Proceedings of the National Academy of Sciences of the United States of America* **97**(17) 9819

[6] Filatov A V, Lekhanov A G and Ubaichin A V (2015) A Microwave radio thermometer for measuring the depth temperatures of biological objects by a noninvasive method *Measurement Techniques* (Article in press) doi: 10.1007/s11018-015-0731-1

[7] Guy A W (1971) Analyses of electromagnetic fields induced in biological tissues by thermographic studies on equivalent phantom models *IEEE Trans. Microwave Theory and Tech.* **19**(2) 205–214

[8] Lin C *et al* (2010) A novel three-fed microstrip antenna for circular polarization application *Journal of Electromagnetic Waves and Applications* **24**(11–12) 1511–1520

[9] Asimakis N P *et al* (2011) Non-invasive microwave radiometric system for intracranial applications: A study using the conformal L-notch microstrip patch antenna *Progress in Electromagnetics Research* **117** 83–101

[10] O'Halloran M, Glavin M and Jones E (2010) *Prog. Electromag. Res*. **107** 203–217

[11] Conceicao R C, O'Halloran M, Glavin M and Jones E (2009) Comparison of planar and circular antenna configurations for breast cancer detection using microwave imaging *Prog. Electromag. Res*. **99** 1–20

[12] Lee J N and Park J K (2010) *Jour. Electromag. Waves Appl.* **24**(2–3,1) 179–188

[13] Corbett R, Laptook A and Weatherall P (1997) *J. Cereb. Blood Flow Metab.* **17**(4) 363–369

[14] Jacobsen S and Klemetsen O (2008) *IEEE Trans. Biomed. Eng.* **55**(12) 2778–2785

[15] Garg R 2001 *Microstrip antennas design handbook* (Norwood, MA 02062)

[16] Kraus J D 1984 *Radio astronomy* (Michigan, Cygnus-Quasar Books)

[17] Filatov A V and Ubaichin A V (2015) *Inst. and exp. tech.* **58**(1) 81–85

[18] Filatov A V, Ubaichin AV and Bombizov A A (2013) *Meas. Tech*. **55**(11) 1281–1286

[19] Filatov A V, Ubaichin A V and Paraev D E (2012) *Inst. Exp. Tech*. **55**(1) 59–64

[20] Filatov AV and Ubaichin A V (2012) *Meas. Tech.* **54** 1–6 doi: 10.1007/s11018-012-9865-6

[21] Ubaichin A V and Filatov A V (2014) *CriMiCo 2014 - 2014 24th International Crimean Conference Microwave and Telecommunication Technology, Conference Proceedings* 928–929